

LIFTING OF DISPERSE PARTICLES FROM A CAVITY BEHIND THE FRONT OF AN UNSTEADY SHOCK WAVE WITH A TRIANGULAR VELOCITY PROFILE

T. R. Amanbaev

UDC 532.529

The gas flow in plane shock waves slipping along an impermeable surface with a rectangular cavity where solid disperse particles are suspended is considered numerically. The motion of the gas and particles (gas suspension) is modeled by equations of mechanics of multiphase media. Some laws of the behavior of the dusty cloud in the cavity are established for the case of wave interaction with the cavity.

Key words: *shock wave, two-phase flow, flow around a cavity.*

The gas flow around cavities is considered in a number of theoretical and experimental works (see, e.g., [1–4]). Unsteady flows in rectangular cavities with a supersonic external flow are considered in [1] within the framework of the ideal compressible gas model. The Euler equations are integrated by Godunov's finite-difference method for Mach numbers $M = 2$ –5 and different width-to-depth ratios of the cavity. The results obtained are compared with available numerical and experimental data. A formula is proposed for the frequency of flow-rate fluctuations in the cavity, depending on the free-stream Mach number and cavity geometry. Unsteady interaction of the shock wave and cocurrent flow with a cavity is experimentally studied in [2]. Based on the analysis of Schlieren and interference patterns and pressure measurements by piezogauges, propagation of a plane shock wave over a shallow rectangular cavity is considered for Mach numbers $M = 1.2$ –5.0. For $M > 4$, spontaneous excitation of oscillations occurs inside the cavity, which is caused by mass exchange between the cavity and external flow (there are no oscillations for $M < 4$).

A series of calculations of a supersonic ($M = 1.03$ –1.30) viscous compressible gas flow around cavities of various depths was performed in [3] on the basis of kinetically correlated difference schemes with a correction. A two-dimensional formulation of the problem with a laminar flow regime was considered. Flows in open and closed cavities were studied. Heat fluxes on the bottom and walls of the cavity were calculated. The flow around a cylindrical cavity on an axisymmetric body was experimentally examined in [4] within the range of Mach numbers $M = 0.60$ –1.18. The effect of the Mach number in passing from subsonic to supersonic flow velocities and the relative aspect ratio of the cavity on flow regimes was considered, including flows with open and closed separation regions. The supersonic turbulent gas flow around rectangular cavities was considered in [5, 6]. The flow in the cavity was simulated by two-dimensional Navier–Stokes equations. In [5], these equations were solved by the MacCormack scheme. It was shown that passive addition of the gas into the cavity can change the flow pattern, transforming a closed cavity into an open one. The flow characteristics and pressure fluctuations depending on the Mach number, relative width of the cavity, and boundary-layer thickness were considered theoretically and experimentally in [6]. The observed disagreement of calculated and experimental values of pressure is explained by the three-dimensional character of the flow in experiments.

At the same time, unsteady gas flows around cavities in shock waves with a triangular velocity profile have not been adequately studied. Apparently, the reason is that unsteady shock waves with a triangular velocity profile refer to the so-called explosive or pulsed type of waves, which are difficult to obtain in experiments.

South-Kazakhstan State University, Shymkent 486050, Kazakhstan. Translated from *Prikladnaya Mekhanika i Tekhnicheskaya Fizika*, Vol. 44, No. 5, pp. 38–44, September–October, 2003. Original article submitted September 30, 2002; revision submitted March 14, 2003.

The present paper deals with numerical simulation of interaction of unsteady shock waves with a cavity containing a cloud of disperse particles.

Equations of Motion and Laws of Phase Interaction. We use the basic assumptions of mechanics of multiphase media [7]. In addition, we assume that the particles are spherical, monodisperse, and incompressible, do not collide with each other, are not split into fragments, and have a constant heat capacity. In specifying the law of particle interaction with the carrier medium, we neglect unsteady forces of virtual mass and buoyancy and Basse forces (this assumption is valid, for instance, if the density of particles is much higher than the density of the gas [7]). The gas is assumed to be ideal and calorically perfect (effects of viscosity and thermal conductivity are manifested only in processes of gas-particle interaction).

Within the adopted assumptions, the equations of plane motion of a two-phase gas suspension of particles have the form [7]

$$\begin{aligned} \frac{\partial \rho_1}{\partial t} + \frac{\partial \rho_1 u_1}{\partial x} + \frac{\partial \rho_1 v_1}{\partial y} &= 0, & \frac{\partial \rho_2}{\partial t} + \frac{\partial \rho_2 u_2}{\partial x} + \frac{\partial \rho_2 v_2}{\partial y} &= 0, \\ \frac{\partial \rho_1 u_1}{\partial t} + \frac{\partial \rho_1 u_1^2}{\partial x} + \frac{\partial \rho_1 u_1 v_1}{\partial y} &= -\frac{\partial p}{\partial x} - n f_x, \\ \frac{\partial \rho_1 v_1}{\partial t} + \frac{\partial \rho_1 u_1 v_1}{\partial x} + \frac{\partial \rho_1 v_1^2}{\partial y} &= -\frac{\partial p}{\partial y} - n f_y, \\ \frac{\partial \rho_2 u_2}{\partial t} + \frac{\partial \rho_2 u_2^2}{\partial x} + \frac{\partial \rho_2 u_2 v_2}{\partial y} &= n f_x, & \frac{\partial \rho_2 v_2}{\partial t} + \frac{\partial \rho_2 u_2 v_2}{\partial x} + \frac{\partial \rho_2 v_2^2}{\partial y} &= n f_y, \\ \frac{\partial \rho_2 e_2}{\partial t} + \frac{\partial \rho_2 u_2 e_2}{\partial x} + \frac{\partial \rho_2 v_2 e_2}{\partial y} &= n q, \\ \frac{\partial}{\partial t} (\rho_1 E_1 + \rho_2 E_2) + \operatorname{div} (\rho_1 E_1 \mathbf{v}_1 + \rho_2 E_2 \mathbf{v}_2 + \alpha_1 p \mathbf{v}_1 + \alpha_2 p \mathbf{v}_2) &= 0, \\ E_i &= e_i + (u_i^2 + v_i^2)/2, & \mathbf{v}_i &= \{u_i, v_i\}, & \mathbf{f} &= \{f_x, f_y\}, \\ p &= \rho_1^0 R_1 T_1, & e_i &= c_i T_i, & \alpha_1 + \alpha_2 &= 1, & \alpha_2 &= n \pi d^3 / 6, \\ \alpha_i &= \rho_i / \rho_i^0, & c_i, R_1, \rho_2^0 &= \text{const}, & i &= 1, 2. \end{aligned}$$

The subscripts 1 and 2 here refer to parameters of the carrier and disperse phases, respectively, ρ_i , ρ_i^0 , \mathbf{v}_i , e_i , E_i , T_i , α_i , and c_i are the reduced and true (marked by the superscript 0) densities, velocity vectors, (u_i and v_i are their components along the x and y axes), internal and total energies, and also temperatures, volume fractions, and heat capacities of the gas and particles, p and R_1 are the gas pressure and the gas constant, n and d are the number of particles in a unit volume of the mixture and their diameter, \mathbf{f} and q are the force of aerodynamic interaction of the gas and particle (f_x and f_y are its components along the x and y axes) and intensity of their heat exchange.

The laws of interphase force and thermal interaction are set in the form

$$\mathbf{f} = (\pi d^2 / 8) \rho_1^0 C_\mu |\mathbf{v}_1 - \mathbf{v}_2| (\mathbf{v}_1 - \mathbf{v}_2), \quad q = \pi d \lambda_1 \text{Nu}_1 (T_1 - T_2),$$

where C_μ is the aerodynamic drag coefficient of the particle, Nu_1 is the Nusselt number, and λ_1 is the thermal conductivity of the gas. For C_μ and Nu_1 , it is usually recommended to use the following semi-empirical relations, which are valid in a wide range of governing parameters [7, 8]:

$$\begin{aligned} C_\mu &= [1 + \exp(-0.423 / M_{12}^{4.63})] (24 / \text{Re}_{12} + 4.4 / \text{Re}_{12}^{0.5} + 0.42), \\ \text{Nu}_1 &= 2 + 0.6 \text{Re}_{12}^{0.5} \text{Pr}_1^{0.33}, & \text{Re}_{12} &= \rho_1^0 d |\mathbf{v}_1 - \mathbf{v}_2| / \mu_1, & \text{Pr}_1 &= c_{p1} \mu_1 / \lambda_1, \\ M_{12} &= |\mathbf{v}_1 - \mathbf{v}_2| / a_1, & a_1 &= \sqrt{\gamma p / \rho_1^0}. \end{aligned}$$

Here Re_{12} , Pr_1 , and M_{12} are the Reynolds, Prandtl, and Mach numbers, μ_1 and c_{p1} are the viscosity and heat capacity (at constant pressure) of the gas, γ and a_1 are the ratio of specific heats and local velocity of sound in the carrier phase.

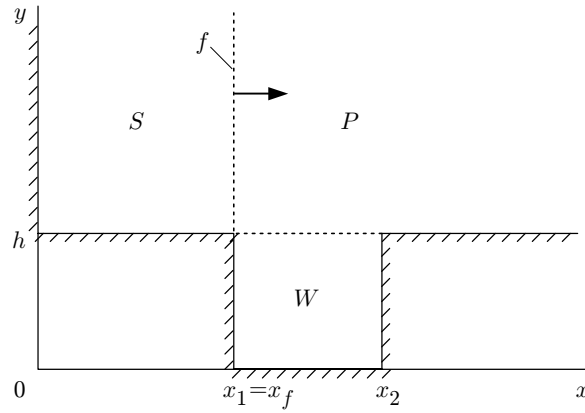


Fig. 1. Diagram of the problem corresponding to the initial time: P is the undisturbed air, W is the cavity filled by a mixture of air and particles, S is the disturbed zone, and f is the shock-wave front.

Initial and Boundary Conditions. The gas parameters ahead of the shock-wave front (marked by the subscript 0) and behind it (marked by the subscript f) are related by the Rankine–Hugoniot equations

$$\rho_{1f}/\rho_{10} = (\gamma + 1)M^2/[2 + (\gamma - 1)M^2],$$

$$u_{1f}/a_{10} = 2(M - 1/M)/(\gamma + 1), \quad p_f/p_0 = (2\gamma M^2 - \gamma + 1)/(\gamma + 1),$$

where M is the Mach number (intensity) of the leading jump (front) of the shock wave. We set the distribution of parameters of the disturbed gas behind the wave front at the initial time $t = 0$, assuming that the velocity profile behind the shock wave is a straight line and the state of the medium is isentropic [7]. Such a distribution of parameters corresponds to a simple Riemann wave at the time of formation of the front shock (discontinuity). Thus, behind the shock-wave front, we have

$$u_1 = u_{1f}x/x_f, \quad v_1 = 0, \quad p = p_f\xi^\gamma, \quad \rho_1 = \rho_{1f}\xi, \quad (x, y) \in S,$$

$$v_1 = 0, \quad p = p_0, \quad \rho_1 = \rho_{10}, \quad \rho_2 = 0, \quad (x, y) \in P,$$

$$v_1, v_2 = 0, \quad p = p_0, \quad \rho_1^0 = \rho_{10}, \quad \rho_2 = \rho_{20}, \quad T_2 = T_{20}, \quad (x, y) \in W,$$

$$S = \{x < x_f, y \geq h\}, \quad P = \{x \geq x_f, y \geq h\}, \quad W = \{x_1 < x < x_2, 0 \leq y \leq h\},$$

$$\xi = [1 - (\gamma - 1)(u_{1f} - u_1)/(2a_{1f})]^{2/(\gamma-1)}.$$

Here h is the depth of the cavity, x_f , x_1 , and x_2 are the coordinates (along the x axis) of the wave front and the front and back boundaries of the cavity, S is the region of the disturbed gas behind the wave, P is the zone above the cavity, and W is the region occupied by the cavity. The scheme of the problem corresponding to the initial time is shown in Fig. 1. We accept the no-slip condition for the gas at the left rigid boundary and on the solid surface and the condition of free outflow for particles, which simulates their deposition on the surface in an absolutely inelastic collision.

Some Calculation Results. The problem posed was solved by a modified method of coarse particles [9, 10]. The calculations were performed by a program developed in the MATLAB environment. The accuracy of calculations was controlled by double recalculation with halved steps in time and coordinates. The optimal step of calculations was established by criteria of stability and necessary accuracy of calculating the processes of interphase interaction.

In addition, to obtain a more detailed flow pattern in regions with strong changes in the medium parameters, where scheme viscosity could be significant, calculations with a grid refined directly inside the cavity and above it were performed. The calculations showed that, for the refinement parameter $r = \Delta x/\Delta x_w = \Delta y/\Delta y_w = 2.4$ (Δx_w and Δy_w are the grid steps in the x and y directions in the regions W and P ; Δx and Δy are the steps in the

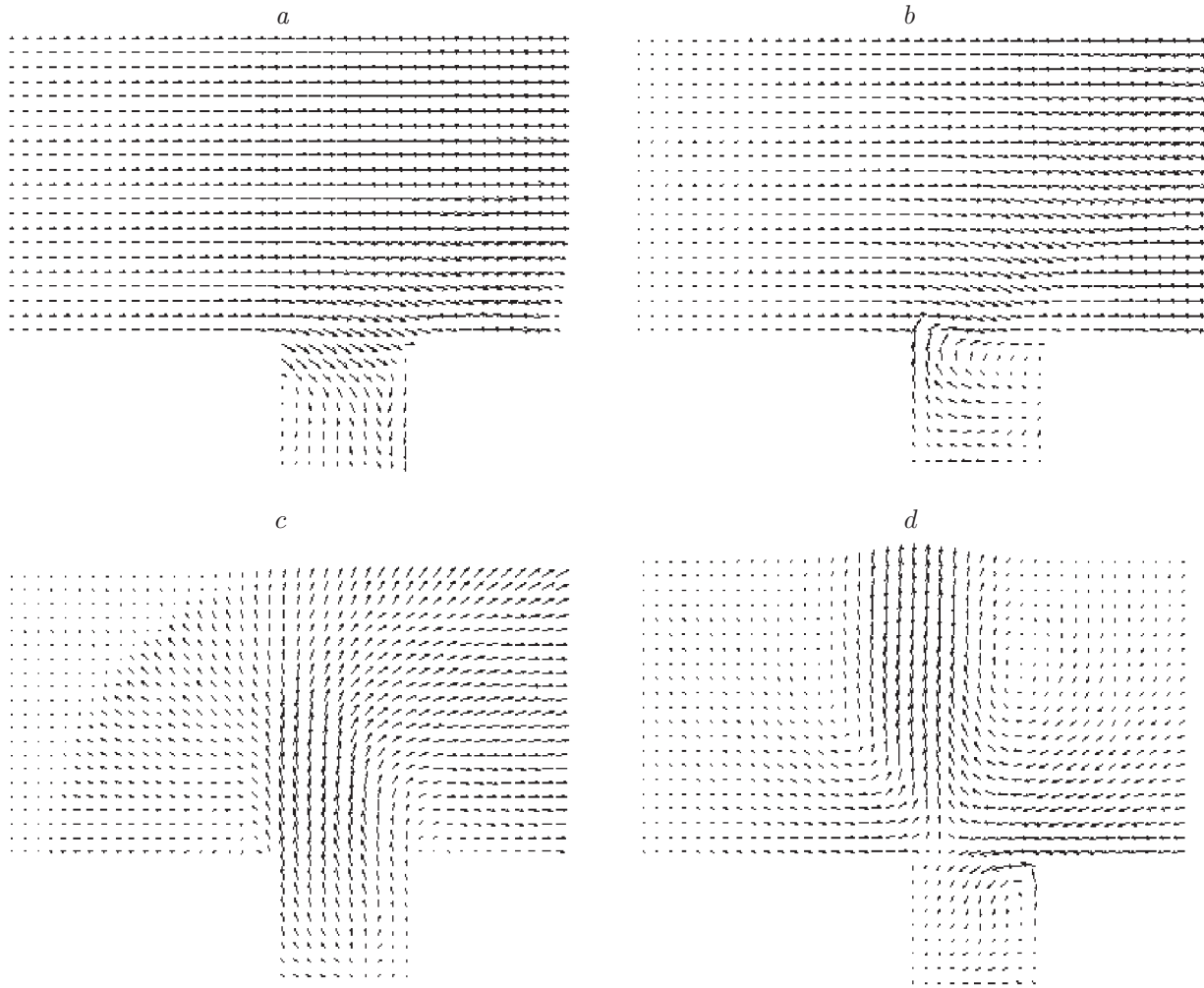


Fig. 2. Field of the velocity vector of the gas for $t = 0.25$ (a), 0.5 (b), 1 (c), and 2 msec (d).

remaining regions of the computational domain), the flow pattern does not experience any significant changes (the difference in parameters was smaller than 1–2%).

Below, we give an example of calculations of the flow behind the shock-wave front with intensity characterized by the Mach number of the leading front $M = 4.2$ and initial pulse length of 0.45 m. The depth h and width l of the cavity with the disperse phase were 0.13 m. At the initial time, the shock-wave front was adjacent to the front boundary of the cavity ($x_f = x_1$). The calculations were performed for air and graphite particles. It was assumed that the disperse and carrier phases in the cavity at the time $t = 0$ were in thermodynamic equilibrium under normal conditions ($p_0 = 0.1$ MPa and $T_{10} = T_{20} = 293$ K). The particle diameter was $d = 60$ μm and the mass fraction of particles in the cavity was $m_2 = \rho_{20}/\rho_{10} = 1$.

Note, depending on the ratio $k = l/h$, there are two flow structures: open and closed. When the parameter k exceeds a certain critical value k_* , the flow becomes attached to the bottom of the cavity (closed structure). For $k < k_*$, a single zone with a circulation flow is formed, i.e., an open structure is observed. In the case of a steady supersonic flow around the cavity, we have $k_* \approx 10$ [4]. In the case considered, the calculation results correspond to the open structure.

Figure 2 shows the field of the velocity vector of the gas at different times. At the times $t = 0.25, 0.5, 1,$ and 2 msec, the shock-wave front is located at a distance from the back edge of the cavity approximately equal to $h, 3h, 7h,$ and $14h$, respectively. At first, when the wave front passes along the cavity, the gas enters the latter with a high velocity. A vortex flow is formed inside the cavity. When the wave goes far ahead, the gas pressure above the

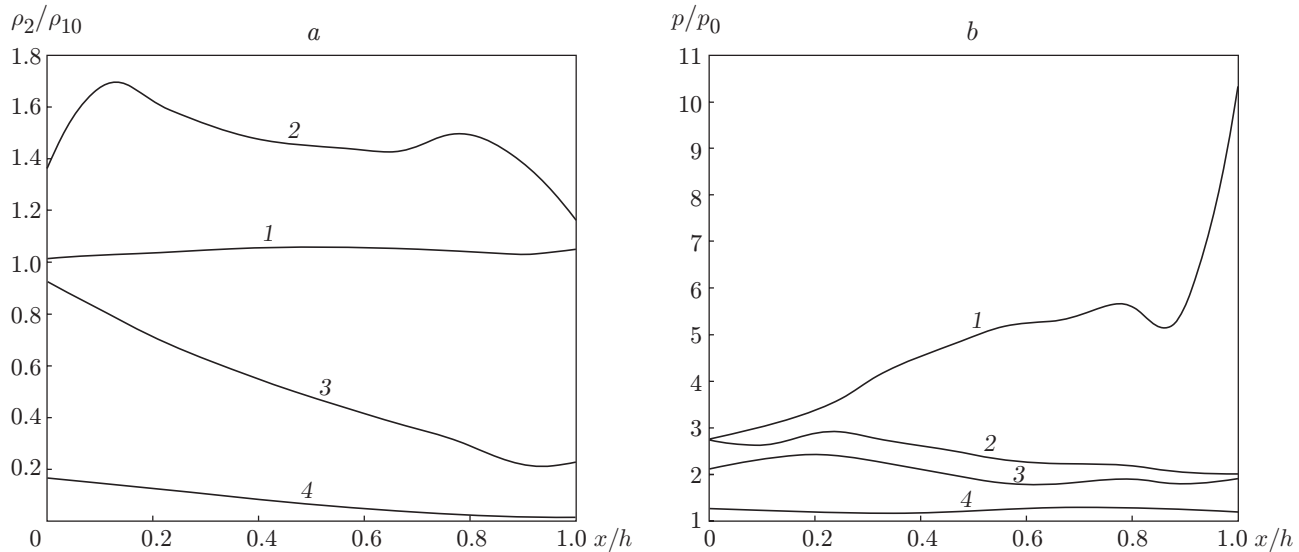


Fig. 3. Distributions of particle density (a) and pressure (b) on the bottom of the cavity for $t = 0.25$ (1), 0.5 (2), 1 (3), and 2 msec (4).

cavity is not very high because of the wave unsteadiness, and the gas moves from the cavity to the main flow region due to the transverse pressure gradient (Fig. 2c). A weak secondary shock wave is formed above the cavity. By the time $t = 2$ msec, a complicated vortex flow is formed above the cavity; near the surface behind the back edge of the cavity, the gas flows in the direction opposite to the wave-front motion and again enters the cavity where a rarefaction region has been already formed (Fig. 2d).

The distribution of the dimensionless reduced density of the disperse phase $\bar{\rho}_2 = \rho_2/\rho_{10}$ over the bottom of the cavity at different times is shown in Fig. 3a. At first, when the gas accelerating behind the wave enters the cavity with a high velocity, the particles move downward under the action of the gas; thus, the zone occupied by the disperse phase is compressed and the particle density significantly increases. In particular, by the time $t = 0.5$ msec, the particle density on the bottom near the front wall is almost 1.7 times higher than the initial value. Note that the distribution of $\bar{\rho}_2$ is nonmonotonic at this time (there are two characteristic maximums near the front and back walls). Later in time, being entrained by the gas flow directed away from the cavity, the particles leave the latter and rise to a significant height. Their density inside the cavity considerably decreases. At the times $t = 1$ and 2 msec, the density of the disperse phase on the bottom near the front wall of the cavity is significantly higher than that near the back wall (curves 3 and 4). By the time $t = 2$ msec, the disperse phase almost completely leaves the cavity.

Figure 3b shows the pressure distribution on the bottom of the cavity. At the time $t = 0.25$ msec, the pressure on the bottom is essentially nonuniform, and it is much higher near the back wall than near the front wall. At later times, when the wave front goes far away from the cavity, the pressure on the bottom is almost uniform and, by the time $t = 2$ msec, it is approximately equal to the initial pressure in the undisturbed gas.

It should be noted that the pressure distribution on the bottom of the cavity in the unsteady case is qualitatively different from the distribution in a steady flow. In the case of unsteady interaction of the shock wave with the cavity, the pressure on the bottom is everywhere higher than the pressure in the undisturbed gas p_0 , whereas a steady flow has a sector behind the front wall where the pressure is lower than p_0 [3, 4].

Thus, it was found that, as the shock wave passes above a dusty cavity, the dust cloud is strongly compressed first under the action of the gas flow entering the cavity. After a certain time (when the wave goes far ahead), the dust particles entrained by the gas flow caused by the transverse pressure gradient rise upward and leave the cavity. A vortex gas flow is formed inside the cavity during a certain time period. In contrast to a steady flow, however, it is transformed into an upward flow with time.

REFERENCES

1. N. L. Zaugol'nikov, M. A. Koval, and A. I. Shvets, "Gas-flow oscillations in cavities in a supersonic flow," *Izv. Akad. Nauk SSSR, Mekh. Zhidk. Gaza*, No. 2, 121–127 (1990).
2. L. G. Gvozdeva, Yu. P. Lagutov, D. K. Raevskii, et al., "Investigation of unsteady stalling flows above cavities," *Izv. Akad. Nauk SSSR, Mekh. Zhidk. Gaza*, No. 3, 185–190 (1988).
3. I. A. Graur, T. G. Elizarova, and B. N. Chetverushkin, "Numerical simulation of the supersonic viscous compressible gas flow around cavities," *Inzh.-Fiz. Zh.*, **61**, No. 4, 570–577 (1991).
4. A. I. Shvets, "Experimental study of flow in a cavity on an axisymmetric body," *J. Appl. Mech. Tech. Phys.*, **42**, No. 2, 262–268 (2001).
5. I. Kim and N. Chokani, "Navier–Stokes study of supersonic cavity flowfield with passive control," *J. Aircraft*, **29**, No. 2, 217–223 (1992).
6. O. Baysal and S. Srinivasan, "Unsteady viscous calculations of supersonic flows past deep and shallow three-dimensional cavities," AIAA Paper No. 88-0101 (1988).
7. R. I. Nigmatulin, *Dynamics of Multiphase Media*, Hemisphere, New York (1991).
8. A. I. Ivandaev, A. G. Kutushev, and R. I. Nigmatulin, *Gas Dynamics of Multiphase Media*, VIVITI, Moscow (1981), pp. 209–291.
9. O. M. Belotserkovskii and Yu. M. Davydov, *Method of Coarse Particles in Gas Dynamics* [in Russian], Nauka, Moscow (1982).
10. A. A. Gubaidullin, A. I. Ivandaev, and R. I. Nigmatulin, "Modified method of coarse particles for calculation of unsteady wave processes in multiphase disperse media," *Zh. Vychisl. Mat. Mat. Fiz.*, **17**, No. 6, 1531–1544 (1977).